ARTICLE

A Novel Silicon Etching Method Using Vapor of TMAH Solution

Jian He[a], Yue-fang Zhao[a], Fang-liang Xu[a,c], Dong-yang Zhao[b], Xiao-juan Hou[a], Xiu-jian Chou[a]*

a. Key Laboratory of Instrumentation and Dynamic Measurement of Ministry of Education, North University of China, Taiyuan 030051, China
b. Beijing Institute of Computer Application, Beijing 100089, China
c. Nanjing Micro-Nano Engineering Research Center, Nanjing 210000, China

(Dated: Received on July 4, 2020; Accepted on August 6, 2020)

Silicon bulk etching is an important part of micro-electro-mechanical system (MEMS) technology. In this work, a novel etching method is proposed based on the vapor from tetramethylammonium hydroxide (TMAH) solution heated up to boiling point. The monocrystalline silicon wafer is positioned over the solution surface and can be anisotropically etched by the produced vapor. This etching method does not rely on the expensive vacuum equipment used in dry etching. Meanwhile, it presents several advantages like low roughness, high etching rate and high uniformity compared with the conventional wet etching methods. The etching rate and roughness can reach 2.13 μm/min and 1.02 nm, respectively. Furthermore, the diaphragm structure and Al-based pattern on the non-etched side of wafer can maintain intact without any damage during the back-cavity fabrication. Finally, an etching mechanism has been proposed to illustrate the observed experimental phenomenon. It is suggested that there is a water thin film on the etched surface during the solution evaporation. It is in this water layer that the ionization and etching reaction of TMAH proceed, facilitating the desorption of hydrogen bubble and the enhancement of molecular exchange rate. This new etching method is of great significance in the low-cost and high-quality MEMS industrial fabrication.

Key words: Silicon bulk etching, MEMS, TMAH solution, Anisotropic etching

I. INTRODUCTION

Etching of silicon as a key process in micro-electro-mechanical system (MEMS) technology, can be generally divided into two categories: dry etching and wet etching. Compared with the dry etching, wet etching has several advantages such as smaller roughness, better uniformity (especially for high aspect ratio microstructures) and lower cost. Moreover, wet etching is the only choice in some cases like 3D structures with slanted sidewalls, batch fabrication. Alkaline solutions like KOH and TMAH (tetramethylammonium hydroxide) are extensively used as etchant. However, so far the best roughness reached by these two etchants is only 5.42 nm due to the formation of pyramid hillocks on etched surface [1−4]. A possible reason is that the hydrogen bubble produced during reaction adheres to the etched surface and acts as a micro-mask [2]. Some researchers use ultrasonic agitation to remove the hydrogen bubbles on the etched surface. Although this method improves the etched surface quality and uniformity, some microstructures like the suspended films, can be easily damaged under the effect of acoustic pressure [5−8]. Zubel *et al.* obtained the low surface roughness and the improved corner undercutting and compensation by introducing various additives into etchants [9−14]. But the introduction of additives decreases the etching rate. Tanaka *et al.* and Tang *et al.* achieved rapid etching of silicon by heating KOH solution to near the boiling point [15, 16]. However, the selectivity between silicon and SiO_2 mask is relatively small (∼150), which is the fatal flaw for back-cavity fabrication. Likewise, the K^+ ion in solution is not compatible with CMOS process, leading to the device failure because of the metal ions contamination to the p-n junction. By contrast, TMAH etchant is compatible with COMS process and has the higher selectivity between silicon and SiO_2 mask despite the lower etch rate and higher roughness. So TMAH is gradually replacing other alkaline solutions as the main etchant in MEMS process [17−20].

In this work, a novel anisotropic vaporous etching method based on the TMAH solution heated up to boiling point has been reported, which avoids the expensive vacuum equipment and possesses the advantages of both wet etching and dry etching. Compared with the traditional wet etching, it increases etching rate of silicon to 2.13 μm/min and decreases the etched surface roughness to 1.02 nm. Meanwhile, the diaphragm structure and Al-based pattern on the non-etched side

*Author to whom correspondence should be addressed. E-mail: chouxiujian@nuc.edu.cn

DOI:10.1063/1674-0068/33/cjcp2007116

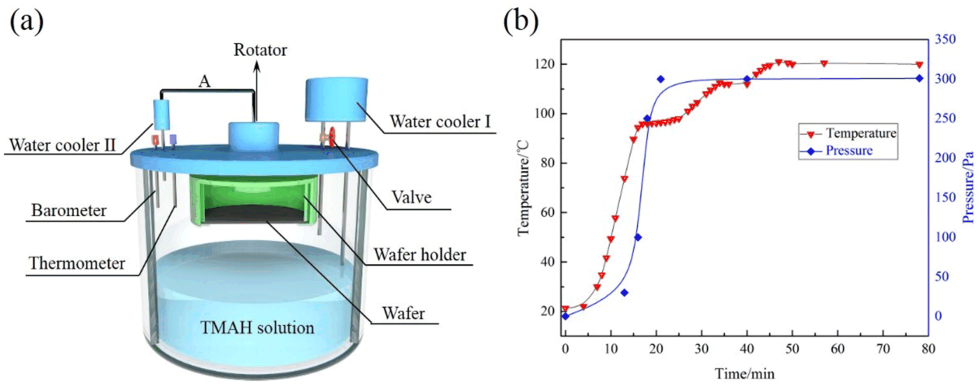

FIG. 1 (a) Schematic diagram of the vaporous etching device based on TMAH etchant. (b) The tendency of temperature and pressure in the etching chamber during heating.

of wafer can be preserved intact without any damage during the back-cavity fabrication.

II. EXPERIMENTS

FIG. 1(a) shows a schematic diagram of equipment for vaporous etching process. The TMAH etchant is gasified by heating the etching chamber. The water cooler I is used to regulate the vapor pressure in the etching chamber. In conventional wet etching process, the diaphragm over cavity is easily damaged by some inevitable factors, such as the vibration of air, the viscous force of liquid. In our case, the target silicon is placed on the polytetrafluoroethylene (PTFE) holder with gasket ring, which is suspended over the liquid surface. In order to protect the device structure on silicon wafer from the internal-external pressure difference, the wafer holder chamber is connected with the outer etching chamber via tube A. Meanwhile, the water cooler II is introduced into this tube to keep TMAH gas in the etching chamber from entering the inner chamber of wafer holder and damaging the device structure on the non-etched side of silicon wafer. Further, the residual etching vapor can be removed by the adsorbing material in the top half of etching chamber. For the sake of etching uniformity, the wafer holder can be rotated at a constant speed by a motor during etching process. Barometer and thermometer are used to monitor the vapor pressure and temperature in the etching chamber, respectively.

The tendency of pressure and temperature in the etching chamber is shown in FIG. 1(b). Measurement shows the boiling temperature of solutions fluctuates between 110 and 115 °C, and the relative gas pressure between 200 and 300 Pa. For the inverted trapezoid micro-pit sample, the 500 μm thick 4-inch (100)-oriented silicon wafers with 500 nm thermal oxidized SiO_2 mask layer are used in this experiment. Considering the depth limitation of focus during the microscope measurement of concave structure, the thickness of wafer and SiO_2 mask layer are 300 μm and 300 nm for the diaphragm samples, respectively. When the etching process is finished, the silicon wafer is washed with deionized water. To verify that the vaporous etching method based on TMAH can prevent the finished device structure on the non-etching side of wafer from being damaged, the Al thin film is fabricated and patterned on the suspended SiO_2 supporting layer, as shown in FIG. S1 (supplementary materials).

III. RESULTS AND DISCUSSION

Etching rate is an important parameter to characterize etching quality. A fast etching rate facilitates cutting down the fabrication time cost and therefore is of great concern in industrial applications. FIG. 2(a) shows the etching rate and surface roughness of Si(100) at different TMAH solution concentrations like 20%, 22%, 25%, 30% and 33%. It can be seen that the etching rate reaches the maximum of 2.13 μm/min at 22%, to our knowledge, which is the highest record for the wet etching based on TMAH [21−24]. As the concentration increases to 33%, the etching rate then slowly decreases to ∼1.5 μm/min. Even so, this value is considerable compared to most of wet etching methods. The high etching rate can be attributed to two factors. On one hand, because of the evaporation process, the exchange rate of molecular between the silicon wafer and the etchant is intrinsically larger than the case in conventional liquid phase etching methods [25]. On the other hand, the higher temperature (boiling point of etching solution) will further speed up the molecular exchange and hence the chemical reactions. In addition, the etching rate uniformity is also important for the identity of MEMS devices during batch fabrication. To examine the uniformity of etching depth, the etched 4-inch wafer is divided into five areas and the average etching depth of Si(100) in every area has been measured, as shown in FIG. 2(b). It can be found that the etching rate uniformity in wafer is less than ±0.8%,

DOI:10.1063/1674-0068/2007116

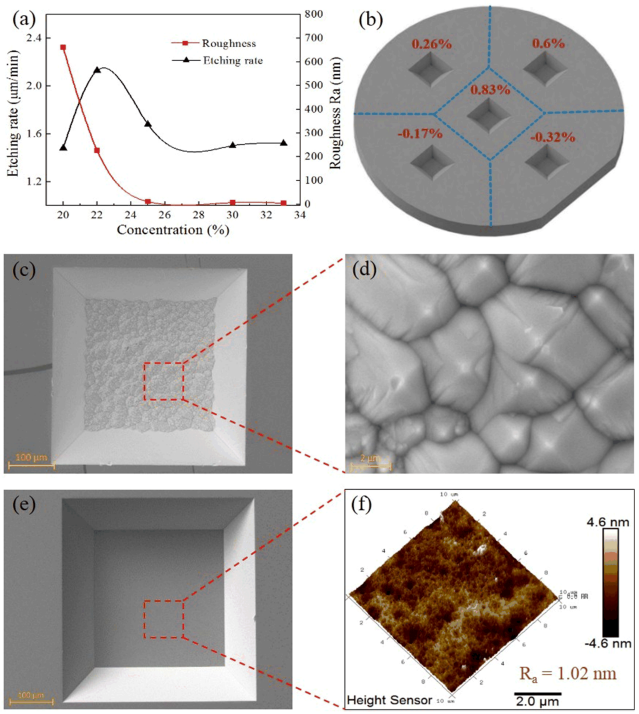

FIG. 2 (a) Etching rate and surface roughness at different TMAH solution concentrations. (b) Schematic diagram of etching uniformity in etched wafer. (c, d) SEM image of etched surface at TMAH concentration of 20%. (e, f) SEM and AFM images of etched surface with concentration of 33%, respectively.

which is much better than that of current dry etching technology [26].

Low etching roughness can suppress the optical loss of optical devices and the contact resistance of electronic device, as well as the detachment of film from it. FIG. 2(a) shows that the surface roughness (measured by step profiler) decreases rapidly with the increasing concentration. When the solution concentration is 20%, the surface roughness reaches hundreds of nanometers. However, when it is 33%, the etched surface roughness is down to 4.5 nm. The trend is consistent with the result obtained by Jun *et al.* [14]. For a visual demonstration of roughness trend, the Si(100) surface is patterned into square and the etched surface morphology is analyzed by SEM and AFM. The typical results are presented in FIG. 2(c−f) (others can be found in FIG. S2 in supplementary materials). The etched surface quality is remarkably improved by the increasing TMAH solution concentration, which echoes the above roughness results from step profiler. For the sample with large roughness at 20% concentration, the surface undulation induced by round hills can be obviously observed by SEM measurement. It is different from the report of Thong *et al.*, where there is no evident undulation outline in etched surface and only horizontally scattered pyramids can be observed [2]. However, it can be seen in small vision

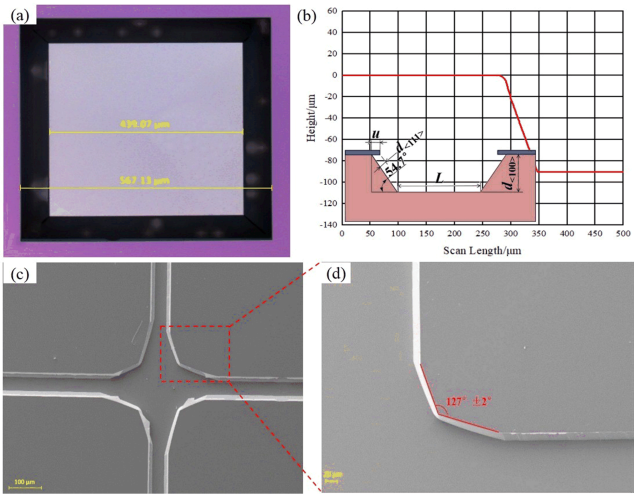

FIG. 3 (a) Optical photograph of sample etched at concentration of 30%. (b) Etch depth measurement by step profiles. (c, d) SEM images of convex corner undercutting under "+" mask.

field that each round hill consists of a large number of micro-pyramids (see FIG. 2(d)). On the contrary, the etched surface of sample of 33% is smooth and the roughness value R_a is 1.02 nm indicated by AFM measurement in area of 100 μm^2 (see FIG. 2(f)).

To gain further insight into the vapor etching technology, another sample is etched at concentration of 30%. As shown in FIG. 3(a), the side length of mask opening on wafer extends from 560 μm to 567.13 μm due to the etching of Si(110). The distance advanced by the sidewall is 7.13 μm, and the bottom width is 439.07 μm. Meanwhile, step meter measurement shows that the etched depth of Si(100) is 90.69 μm (FIG. 3(b)). As we know, the angle θ between Si(111) and Si(100) in wet anisotropic etching is 54.7°. Consequently, it can be derived that Si(111) etched depth is 2.9 μm. The Si(100) etched depth $d_{\langle 100\rangle}$ can be calculated by

$$d_{\langle 100\rangle} = \frac{(2u + W - L)}{2} \tan\theta \qquad (1)$$

where W is the window width of the mask, L is the bottom width, u is lateral undercutting. The obtained result is 90.4 μm, which is consistent with the above experimental value. Besides, it can be calculated that Si(111)/Si(100) etching ratio is 31.17. It implies that the etched profile in vapor etching is identical to the counterpart in conventional wet etching methods. In addition, the SiO_2 mask thickness is reduced by 40 nm after the silicon wafer is etched by about 90 μm along (100) orientation (see FIG. S3 in supplementary materials). The selectivity ratio of Si/SiO_2 can be calculated to 1456, which is lower than that of liquid TMAH etching (∼5000 [27]), but higher than that of liquid KOH etching (∼150 [21]). So, if one needs to etch through a silicon wafer of 500 μm thickness from one side of the

DOI:10.1063/1674-0068/2007116

wafer, a SiO_2 film of 300 nm thickness is enough for the etching mask. FIG. 3(c) gives the etched pattern wafer under "+" mask. Similarly to conventional wet etching methods, the convex corner undercutting phenomenon is observed. The included angle of the undercut edges is ∼127±2°. It differs from results in TMAH wet etching, where the angle is 140°±2° [21]. An appropriate result (∼127°±2°) has been observed by Wu *et al.* in wet etching based on hydrazine, KOH and EPW (ethylenediamine-pyrocatechol-water), in which the main beveling planes at undercut corner are {212} planes [27]. So, the convex corners undercutting is because the {212} planes etch faster than others, resulting in a loss of the desired structure.

Diaphragm is used in many MEMS applications like film bulk acoustic resonator, infrared radiation source [23]. In the practical wet etching process, diaphragm is easily torn by agitation, ultrasound and etching liquor adhesion induced by surface tension [6], resulting in the low yield. In this work, the etching reaction occurs on the solid-gas interface, rather than the solid-liquid interface. Also, the agitation or ultrasound is circumvented by the rotation of sample holder. Moreover, there is an internal-external pressure balance design in our equipment. So, when the back-cavity etching is self-stopped, the SiO_2 diaphragm with 300 nm thickness can be preserved intact without any ruptures (FIG. 4(a)). Compared with the diaphragm from dry etching method (FIG. 4(b)), the pattern from vaporous anisotropic etching is more regular and the boundary line is sharper. Al is a technologically important material in MEMS process, which is usually used as electrode or buffer layer. However, it is chemically active and thus easily attacked during wet etching. In our vaporous etching method, the wafer side with Al microstructure can be protected by sealing it in the PTFE holder with gasket ring, which is the advantage similar to dry etching. FIG. 4 (c) and (d) gives the SEM images of the sample with pentagon Al electrode of 200 nm thickness. It can be seen that Al electrode pattern is not damaged after the back-cavity etching is finished.

According to the above experimental results, the possible reaction mechanism of vaporous anisotropic etching based on TMAH etchant can be analyzed. Typically, the etching mechanism of silicon in alkaline etchant is investigated by measuring the H/D-kinetic isotopic effect on dissolution rate [28−31]. The rate determining step is the breaking of Si−H bond. After the alkaline solute is ionized, the reaction sequence is initiated by the OH^- catalyzed attack of Si−H by H_2O through the formation of an intermediate. It is generally accepted that the fracture of the Si−H bond catalyzed by OH^- ion is a nucleophilic substitution reaction, which contains the following two steps [21]:

Oxidation

$$(\equiv Si)_3SiH+OH^-+H_2O\rightarrow(\equiv Si)_3SiOH+H_2+OH^- \quad (2)$$

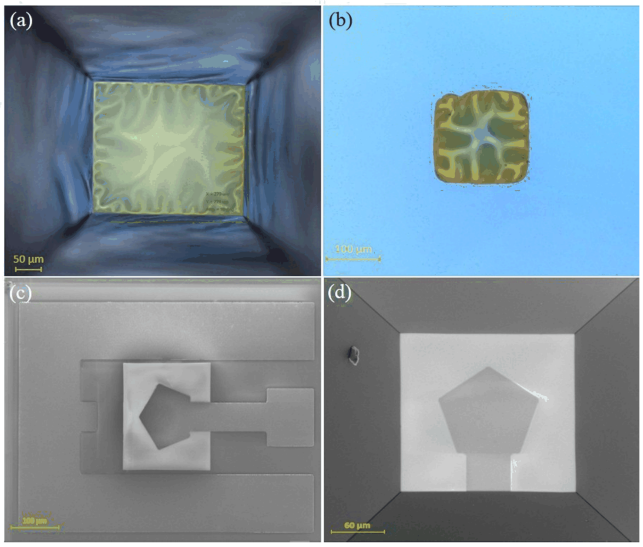

FIG. 4 Optical photograph of diaphragm etched by (a) vaporous etching and (b) dry etching, the SEM image of (c) front microstructure and (d) self-stopped back-cavity structure with pentagonal Al electrode.

Etching

$$(\equiv Si)_3SiOH+3H_2O \rightarrow 3(\equiv SiH)+Si(OH)_4 \quad (3)$$

In our case, the tendency of etching rate and roughness, the etching profile and the convex corner undercutting are similar to the liquid TMAH etching situation. Likewise, the energy dispersive spectrum reveals that the Si/O ratio in by-product is ∼0.5 (FIG. S4 in supplementary materials), which is consistent with the report of Lai *et al.* about the aqueous TMAH etching method [32]. Therefore, it can be inferred that the etching reaction in this work to a large extent is identical to the conventional aqueous phase situation. But what is different is that a water thin film will be formed on the etched surface during the solution evaporation. The ionization of TMAH molecular and the etching reaction of silicon wafer occur in this water layer (Noting that the gas temperature is ∼110 °C, which is lower than the decomposition temperature 130 °C of TMAH [33]). The etching reaction process can be illustrated in FIG. 5. On one hand, the generated by-product H_2 bubble in the water thin film is easier to desorption from the etched surface in the absence of liquid pressure and surface tension. Hence, the micro-mask effect can be eliminated and then a smooth etched surface can be achieved. The large roughness at low concentration is possibly because of the increasing randomness of OH^- distribution in gas and the non-uniform removal of atoms from the surface or lattice defects. On the other hand, the high etching rate probably originates from the high molecular exchange rate and the high etching temperature, as mentioned above. However, with the increasing of solution concentration, the adsorption of

DOI:10.1063/1674-0068/2007116

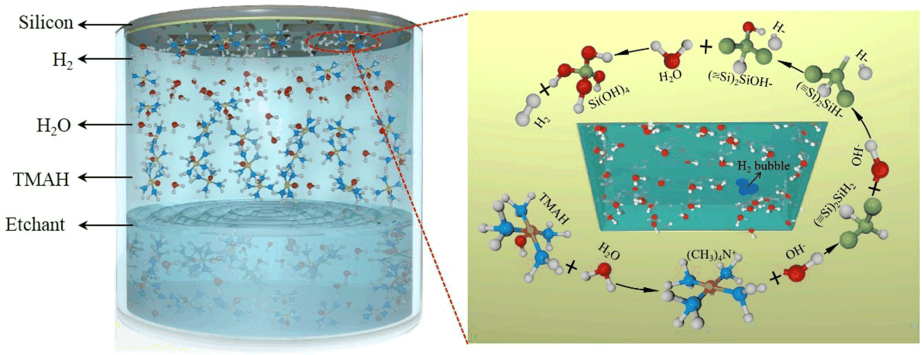

FIG. 5 Etching reaction mechanism.

cation TMA^+ on silicon surface with a particular orientation is enhanced due to the similar structure and diameter to silicon tetrahedral [34]. It will suppress the adsorption of OH^- and the breaking of Si−H bond, reducing the etching rate. In addition, as the roughness decreases at higher solution concentration, the number of dangling bonds on etched surface decreases, which further reduces the adsorption of OH^- and the etching rate. Therefore, the experimental results shown in FIG. 2 has been observed.

IV. CONCLUSION

In this work, a novel vaporous etching method is proposed based on TMAH etchant, in which the TMAH solution is heated up to boiling point and the wafer is positioned over the liquid surface. Compared to the conventional TMAH wet etching, this method can achieve high-quality efficient vaporous anisotropic etching of monocrystalline silicon. Meanwhile, it has several advantages like low roughness, high etching rate, and high uniformity. Moreover, the diaphragm structure and Al-based pattern on the non-etched side of wafer can be preserved intact without any damage during the back-cavity fabrication. Based on the obtained experimental result, the corresponding etching mechanism is proposed. It is indicated that a water thin film will be formed on the etched surface during the solution evaporation, in which the ionization and etching reaction of TMAH proceed, facilitating the desorption of hydrogen bubble and the enhancement of molecular exchange rate. This new type of etching method is of great significance in the low-cost and high-quality MEMS industrial fabrication.

Supplementary materials: The technological process for making Al graphics on SiO_2 diaphragm, the SEM images of etched samples at different concentrations, the step profilers of SiO_2 mask layer thickness and the energy dispersive spectrum of by-product are available.

V. ACKNOWLEDGMENTS

The work was supported by the National Natural Science Foundation of China (No.51675493, No.51975542), the National Key R&D Program of China (No.2018YFF0300605, No.2019YFF0301802, No.2019YFB2004802), Program for the Outstanding Innovative Teams of Higher Learning Institutions of Shanxi and Shanxi "1331 Project" Key Subject Construction (1331KSC).

[1] L. M. Landsberger, S. Naseh, M. Kahrizi, and M. Paranjape, J. Microelectromech. Syst. **5**, 106 (1996).
[2] J. T. L. Thong, P. Luo, W. K. Choi, and S. C. Tan, J. Micromech. Microeng. **11**, 61 (2001).
[3] J. S. You, D. Kim, J. Y. Huh, H. J. Park, J. J. Pak, and C. S. Kang, Solar Energy Mate. Solar Cells **66**, 37 (2001).
[4] J. T. L. Thong, Y. Bai, P. Luo, and W. K. Choi, Mater. Sci. Eng. B **72**, 177 (2000).
[5] W. S. Che, C. G. Suk, T. G. Park, J. T. Kim, and J. H. Park, Key Eng. Mater. **297-300**, 557 (2005).
[6] C. R. Yang, P. Y. Chen, Y. C. Chiou, and R. T. Lee, Sens. Actuators A Phys. **119**, 263 (2005).
[7] K. Ohwada, Y. Negoro, Y. Konaka, and T. Oguchi, Sens. Actuators A Phys. **50**, 93 (1995).
[8] J. Chen, L. T. Liu, Z. J. Li, Z. M. Tan, Q. S. Jiang, H. J. Fang, Y. Xu, and Y. X. Liu, Sens. Actuators A Phys. **96**, 152 (2002).
[9] C. R. Yang, P. Y. Chen, C. H. Yang, Y. C. Chiou, and R. T. Lee, Sens. Actuators A Phys. **119**, 271 (2005).
[10] I. Zubel and M. Kramkowska, Sens. Actuators A Phys. **101**, 255 (2002).
[11] K. B. Sundaram, A. Vijayakumar, and G. Subramanian, Microelectron. Eng. **77**, 230 (2005).
[12] D. Resnik, D. Vrtacnik, U. Aljancic, and S. Amon, J. Micromech. Microeng. **13**, 26 (2003).
[13] P. Pal, M. A. Gosálvez, and K. Sato, J. Micromech. Microeng. **22**, 065013 (2012).
[14] K. H. Jun, B. J. Kim, and J. S. Kim, Electron. Mater. Lett. **11**, 871 (2015).

DOI:10.1063/1674-0068/2007116

[15] H. Tanaka, S. Yamashita, Y. Abe, M. Shikida, and K. Sato, Sens. Actuators A Phys. **114**, 516 (2004).
[16] B. Tang, K. Sato, D. Zhang, and Y. S. Cheng, Micro Nano Lett. **9**, 582 (2014).
[17] K. Biswas and S. Kal, Microelectron. J. **37**, 519 (2006).
[18] K. Tokoro, D. Uchikawa, M. Shikida, and K. Sato, *Proceedings of the 1998 International Symposium on Micromechatronics and Human Science*, Nagoya, Japan, (2002).
[19] A. B. Anoop Prakash, J. G. Jency, and M. C. Mathew, *IJCA Proceedings on International Conference on Innovations in Intelligent Instrumentation*, Optimization and Electrical Sciences, (2013).
[20] O. Tabata, R. Asahi, H. Funabashi, K. Shimaoka, and S. Sugiyama, Sens. Actuators A Phys. **34**, 51 (1992).
[21] P. Pal and K. Sato, *Silicon Wet Bulk Micromachining for MEMS*, Singapore: Jenny Stanford Publishing, (2017).
[22] Y. J. Fan, P. D. Han, P. Liang, Y. P. Xing, Z. Ye, and S. X. Hu, Appl. Surf. Sci. **264**, 761 (2013).
[23] V. Swarnalatha, A. V. Narasimha Rao, A. Ashok, S. S. Singh, and P. Pal, J. Micromech. Microeng. **27**, 085003 (2017).
[24] I. Zubel, J. Micromech. Microeng. **29**, 093002 (2019).
[25] M. Kalb, T. Kluge, H. Eckhardt, A. Weise, I. Prokhorov, M. Kraml, E. Eiche, and T. Neumann, Geochim. Cosmochim. Acta **269**, 167 (2020).
[26] R. Barnett, D. Thomas, Y. P. Song, D. Tossell, T. Barrass, and O. Ansell, *Proceedings of the 60th Electronic Components and Technology Conference*, Las Vegas, NV, USA, 1056 (2010).
[27] X. P. Wu and W. H. Ko, Sens. Actuators **18**, 207 (1989)
[28] T. Baum and D. J. Schiffrin, J. Electroanal. Chem. **436**, 239 (1997).
[29] S. A. Campbell, D. J. Schiffrin, and P. J. Tufton, J. Electroanal. Chem. **344**, 211 (1993).
[30] O. J. Glembocki, E. D. Palik, G. R. de Guel, and D. L. Kendall, J. Electrochem. Soc. **138**, 1055 (1991).
[31] P. M. M. C. Bressers, S. A. S. P. Pagano, and J. J. Kelly, J. Electroanal. Chem. **391**, 159 (1995).
[32] C. Lai, X. M. Li, L. K. Zou, Q. Chen, B. Xie, Y. L. Li, X. L. Li, and Z. Tao, Corros. Sci. **85**, 471 (2014).
[33] C. Zhou, J. M. Li, L. Wu, G. R. Guo, H. B. Wang, P. Chen, B. J. Yu, and L. M. Qian, RSC Adv. **8**, 36043 (2018).
[34] Z. Irena, Sens. Actuators A Phys. **303**, 111829 (2020).

DOI:10.1063/1674-0068/2007116